WEP Warwick Evans Publishing

International Journal of Materials Science and Technology Studies

ISSN: 3006-7693 (Print), ISSN: 3006-3744 (Online) | Volume 1, Number 1, Year 2024
DOI: https://doi.org/10.62051//ijmsts.v1n1.07
Journal homepage: https://wepub.org/index.php/IJMSTS/index

Study on the corrosion inhibition performance of Schiff base corrosion inhibitor on Q235 steel

Zixi Zhao, Xiumei Wang*

School of Materials Science and Engineering, Shenyang Jianzhu University, Shenyang, China
*Corresponding Author: xmwang@alum.imr.ac

ABSTRACT

Q235 steel is widely used in industry and daily life, and it is prone to corrosion during use, especially in hydrochloric acid solution where corrosion is particularly severe. Schiff base organic compounds can significantly inhibit the corrosion of Q235 steel in hydrochloric acid solution, making them a green and environmentally friendly organic compound. This article uses aniline, octadecylamine, and glutaraldehyde as raw materials to prepare two Schiff base corrosion inhibitors, namely bisaniline Schiff base and bisoctadecylamine Schiff base (named BXFJ and SXFJ respectively). The corrosion inhibition performance and mechanism of these two Schiff base inhibitors in Q235 steel in hydrochloric acid solution were studied using weight loss method, electrochemical testing, quantum chemical theory calculation, and molecular dynamics simulation. The results of weight loss method and electrochemical testing show that in a 1mol/L HCl solution, the corrosion inhibition performance of BXFJ at a concentration of 25mg/L is higher than that of SXFJ, indicating that BXFJ can exert excellent corrosion inhibition performance in HCl environment. Density functional theory (DFT) indicates that the active sites of the two Schiff bases are C=N double bonds, and molecular dynamics (MD) further confirms that both Schiff base corrosion inhibitors can adsorb on the surface of Q235 steel.

KEYWORDS

Weightlessness method; Electrochemical testing; Quantum chemical calculations; Molecular dynamics simulation; Schiff base corrosion inhibitor

1. INTRODUCTION

The harm of corrosion is astonishing for human life and industrial development. It is estimated that about one-third of the annual production of steel produced in the industrial world is scrapped due to corrosion. To solve the problem of corrosion, developed countries spend 3% to 4% of their GDP annually. This is only a direct economic loss caused by corrosion, while the indirect damage caused by corrosion is more extensive and severe. For example, stress corrosion fracture can lead to aircraft crashes, turbine blades flying apart, and bridge collapses. Therefore, metal protection work is imperative, and selecting corrosion inhibitors to protect metal products is the most economical and effective method. The commonly used corrosion inhibitors include inorganic salts such as nitrite, phosphate, polyphosphate, carbonate, silicate, borate, chromate, etc. [2], but they are highly toxic and can cause eutrophication of water, and have been banned. Some organic compounds containing heteroatoms such as P, O, N, S, and π bonds, aromatic rings, and heterocycles have the characteristics of low toxicity and high efficiency, and are widely used as corrosion inhibitors to inhibit metal corrosion [3-6]. Excellent corrosion inhibitors are organic compounds containing conjugated double bonds, heteroatoms (i.e. sulfur, nitrogen, oxygen, phosphorus), aromatic rings, and other structures. Among them, Schiff base corrosion inhibitors have many advantages such as simple synthesis, green

and non-toxic, and have important applications in the fields of medicine, catalysis, analytical chemistry, and corrosion. After in-depth research, Schiff base has the potential to become an efficient corrosion inhibitor for carbon steel in acid pickling solutions [7]. Schiff base corrosion inhibitors are organic corrosion inhibitors that have a wide range of biological activities due to their unique conjugated structure. They can coordinate with metals and adsorb on metal surfaces to form a film, playing a corrosion inhibition role. Organic compounds with excellent corrosion inhibition performance usually contain heteroatoms or π bonds. Heteroatoms such as N and O containing lone pair electrons can form bonds with metals and adsorb on the metal surface, providing corrosion protection; The bonds in compounds exhibit excellent corrosion inhibition performance due to the interaction between their orbitals and metals. Schiff base compounds contain C=N double bonds and often contain benzene rings and several heteroatoms, making them highly susceptible to adsorption with metals and exhibiting excellent corrosion inhibition behavior.

2. EXPERIMENTAL

2.1. Theoretical Model

This article selects two types of Schiff base corrosion inhibitors, namely bisaniline Schiff base (BXFJ) and bisoctadecylamine Schiff base (SXFJ). The molecular structures are shown in Figure 1.

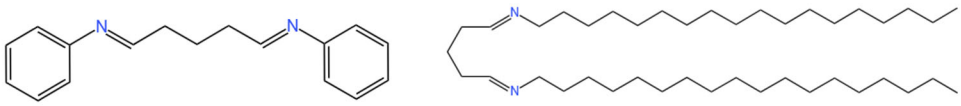

(a) (b)

Figure 1. Molecular structure: (a) BXFJ; (b) SXFJ

2.2. Weightlessness method

The experimental material used for the weight loss method in this article is Q235 steel, and the corrosive medium used is a 1mol/L HCL solution.

Experimental steps:

(1) Grind Q235 steel smoothly on a metal grinder using 80 #, 100 #, and 800 # water-resistant sandpaper in sequence, then clean with distilled water and anhydrous ethanol, blow dry with cold air, and dry in an electric hot air drying oven for more than 4 hours. After the test block is completely dry, weigh it on a balance and record it in sequence. Use a digital caliper to measure the length, width, and height of the test piece and record it in sequence.

(2) Weigh different concentrations and types of Schiff base corrosion inhibitor solutions using pipettes, add them to 1mol/l hydrochloric acid solution (diluted with distilled water), and pour them into a conical flask. Hang the test blocks with a fishing line in 200mL of corrosion test solution, and place three test blocks in each beaker to ensure that the test blocks are completely immersed in the corrosion solution. Change the concentration of corrosion inhibitor, reaction temperature, reaction time and other conditions, and repeat the above experiment.

(3) After removing the test piece, rinse the surface with distilled water and anhydrous ethanol in sequence. Then, use a degreased cotton dipped in acid solution to wipe off the corrosion products on the surface of the test piece. Finally, rinse again with anhydrous ethanol and blow dry with cold air. After complete drying, weigh the weight using an electronic balance. The average corrosion rate V of Q235 steel under different conditions and the quality corrosion inhibition efficiency of Schiff base corrosion inhibitors η It can be calculated separately according to equations (1) and (2).

$$V = \frac{8.76 \times 10000 \times \Delta m}{S * t * \rho} \quad (1)$$

In the formula, V is the average corrosion rate, g · cm^{-2} · h^{-1}; Δm is the difference in sample mass between before corrosion and after reaction, g; S is the total exposed area of the sample, ^{cm2}; ρ *The* density of the sample participating in the reaction, g · ^{cm3}; T is the total reaction time, h.

$$\eta = \frac{m_0 - m}{m_0} \quad (2)$$

In the formula, η Quality corrosion inhibition efficiency, (%); $_{M0}$ and m are the masses of corrosion products extracted from Q235 steel before and after corrosion, respectively.

2.3. Electrochemical testing

Electrochemical testing uses a CHI660E workstation to measure the electrochemical impedance spectrum and dynamic potential polarization curve. A three electrode working system is used, with Q235 steel electrode as the working electrode, platinum plate electrode as the auxiliary electrode, and saturated calomel electrode as the reference electrode. Before conducting electrochemical testing, the Q235 steel electrode needs to be immersed in an electrolyte (250 mL of test solution containing different concentrations of corrosion inhibitors) for half an hour to obtain a stable open circuit potential (OCP). After the open circuit potential stabilizes, impedance testing (EIS) is performed, with a scanning frequency range of 0.01~100 kHz and a perturbation voltage of 20 mV. Zview software is used to fit EIS data to obtain corresponding impedance parameters and equivalent circuits. The scanning range of the dynamic potential polarization curve is set to $_{EOCP}$ ± 250 mV, and the scanning rate is set to 0.1 mV/s. Calculate the corrosion inhibition efficiency based on equations (3) and (4) from the polarization curve and impedance test results.

$$\eta_p(\%) = \frac{I^0_{coor} - I_{coor}}{I_{coor}} \times 100\% \quad (3)$$

In the formula, ^{I0coor} and $_{Icorr}$ are the corrosion current densities of Q235 steel measured without and with added corrosion inhibitors, respectively; MA · $^{cm-}$2.

$$\eta_e(\%) = \frac{R_{ct} - R^0_{ct}}{R_{ct}} \times 100\% \quad (4)$$

In the formula, ^{R0t} and $_{Rt}$ are the charge transfer resistances at the interface of Q235 steel solution measured without and with added corrosion inhibitors, Ω · ^{cm2}, respectively.

2.4. Quantum chemical calculations

Quantum chemistry research is based on the fundamental laws of electronic motion, simulating the electron nucleus system through calculations, and integrating the Schr ö dinger equation. Nowadays, people use various computational models, such as Ab initio Method [8], Semi empirical Method [8], Density Function Theory, DFT [10], etc. Although they are different, they are all based on approximate computational foundations.

The molecular configurations of corrosion inhibitors were all created in the Materials Studio software MS Visualizer. In order to obtain the most stable molecular configuration, the DMol3 module was used for structural optimization. The global reaction activity parameters obtained through quantum chemistry calculations after optimization, including the highest occupied molecular orbital energy ($_{EHOMO}$), lowest empty molecular orbital energy ($_{ELUMO}$), and hardness(η), Softness (S), energy gap(hello) dipole moment (μ) Characterized the reactivity of molecules.

Calculation formula:

$$\Delta E = E_{\mathrm{LUMO}} - E_{\mathrm{HOMO}} \quad (5)$$

$$\mu = \frac{1}{2}(E_{\mathrm{HOMO}} + E_{\mathrm{LUMO}}) \quad (6)$$

$$\eta_a = \frac{1}{2}(E_{\mathrm{LUMO}} - E_{\mathrm{HOMO}}) \quad (7)$$

$$S = \frac{1}{\eta} \quad (8)$$

2.5. Molecular Dynamics Simulation

Molecular dynamics simulation can provide a better understanding and description of substances. Build a molecular model of the corrosion inhibitor using the Visualizer module in Materials Studio software, then construct a Fe crystal model and establish a simulation system. Use the Focrite module for geometric optimization, use the Geometry Optimization option in the Forcite module, simulate selecting the Dynamics option in the Forcite module, select Fine for accuracy, and select COMPASS II for force field. The NVT system is selected for the system, with an initial speed of Random and a simulated temperature of 25℃ (298K). The temperature is controlled using an Anderson thermostat. This article simulates the adsorption behavior of Schiff base corrosion inhibitors in vacuum.

The simulation system consists of Fe (100) surface, 1 corrosion inhibitor molecule, and a vacuum layer. Firstly, import the metal Fe lattice, optimize the lattice using the DMol3 module, cut out the Fe (100) surface, select U=12 and V=12, establish a supercell, establish a vacuum layer with a thickness of 70 Å, add a corrosion inhibitor molecule into the constructed system, adjust the position of the inhibitor molecule, and make the molecular head base perpendicular to the Fe surface. Fix all Fe atoms again, and finally optimize the constructed system in the force module by selecting Geometry optimization and using a compass force field. Then perform molecular dynamics simulations on the system, select the NVT ensemble, set the temperature to 298k, simulate a total time of 1000ps, and output a total of 10000 trajectory files.

The formula for calculating adsorption energy is as follows:

$$E_{\mathrm{adsorption}} = E_{\mathrm{total}} - (E_{\mathrm{molecule}} + E_{\mathrm{surface}}) \quad (9)$$

Among them: $E_{adsorption}$: the adsorption energy of the system;

Etotal: The total energy of the system after 120ps simulation;

Emolecule: the energy of corrosion inhibitor molecules;

Esurface: The energy of the Fe (100) surface.

3. RESULTS AND DISCUSSION

3.1. Results of Weightlessness Method

Measure the corrosion inhibition performance of two different concentrations of Schiff bases on Q235 steel in a 1mol/L HCl solution under temperature conditions of 4 hours and 30℃, with average corrosion rate V and mass corrosion inhibition efficiency η, The specific calculation formulas are shown in (1) and (2).

The test results are shown in Figure 2:

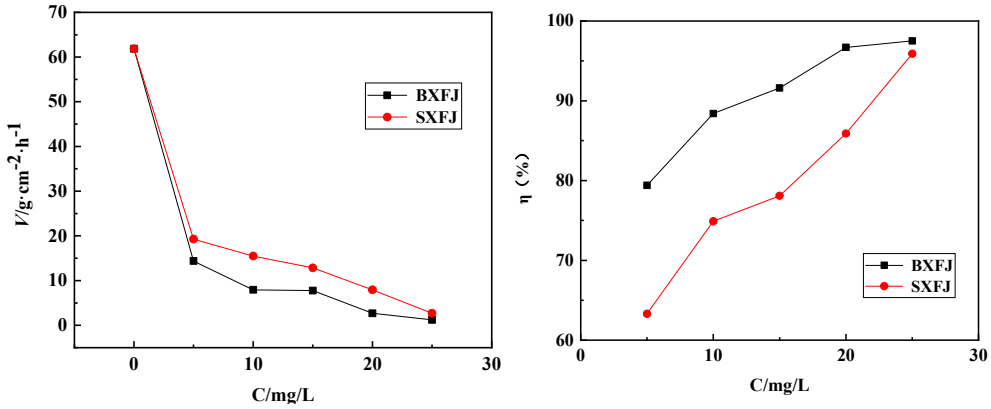

(a) (b)

Figure 2. Relationship between the concentration of Schiff base corrosion inhibitor and the corrosion efficiency

During the experiment, it was observed that a large number of bubbles were generated on the surface of carbon steel in blank hydrochloric acid, while in the hydrochloric acid solution containing two Schiff base corrosion inhibitors, the bubbles on the surface of carbon steel were significantly reduced. After the experiment, the carbon steel in the blank hydrochloric acid showed black color and obvious corrosion pits, with many corrosion products on the surface, indicating that the carbon steel was severely corroded by hydrochloric acid; At the same time, the surface of carbon steel in hydrochloric acid with Schiff base corrosion inhibitor is relatively intact and bright, and there is no occurrence of pitting corrosion, resulting in fewer surface corrosion products. Through surface observation, it can be preliminarily inferred that the addition of Schiff base corrosion inhibitors has an inhibitory effect on the corrosion of metals.

As shown in the figure, with the increase of corrosion inhibitor concentration, the corrosion rate decreases and the corrosion inhibition rate increases. And when the concentration of the corrosion inhibitor is 25mg/L, the two Schiff base corrosion inhibitors have the best corrosion inhibition effect.

3.2. Electrochemical Curve Results

At room temperature, test the potentiodynamic polarization curves of Q235 steel electrodes in blank and hydrochloric acid solutions with different concentrations (5, 15, 25mg/L) of BXFJ and SXFJ added. The results are shown in Figure 3, and the corrosion potential (E_{corr}), corrosion current density (I_{corr}), and Tafel slope (ba and b_c) are obtained by extrapolating the Tafel line from Figure 3. The corrosion inhibition efficiency is calculated using formula (3). The electrochemical parameters are listed in Table 1.

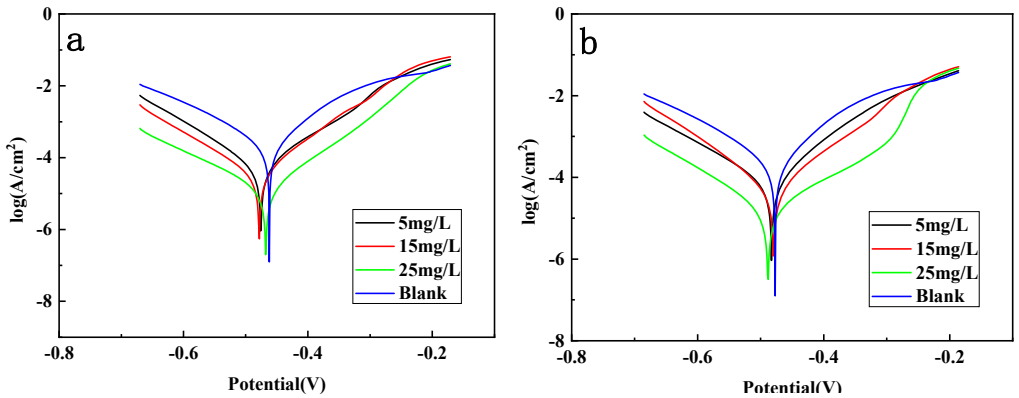

Figure 3. Electrodynamic polarization curve of Q235 steel in 1 M HCl solution with different concentration of corrosion inhibitor. (a) BXFJ; (b) SXFJ

Table 1. Electrical parameters of Q235 steel in 1 M HCl solution with different concentrations of corrosion inhibitors

Corrosion inhibitor	concentration(mg·L-1)	Ecoor (V)	Icoor (mA·cm-2)	bc (V·dec-1)	ba (V·dec-1)	ηp(%)
blank	0	-0.482	238.4	8.11	11.321	-
BXFJ	5	-0.486	51.85	10.831	11.959	78.25%
	15	-0.488	33.46	10.115	13.85	85.96%
	25	-0.484	14.51	8.169	11.511	93.91%
SXFJ	5	-0.483	72.8	8.827	13.157	69.46%
	15	-0.483	54.06	10.112	10.676	77.32%
	25	-0.484	19.06	8.792	9.773	92.01%

From Figure 3 and Table 1, it can be seen that after the addition of BXFJ and SXFJ, the corrosion potential $_{Ecoor}$ of Q235 steel is all negatively shifted, indicating that BXFJ and SXFJ are mixed corrosion inhibitors. As shown in Figure 3, the curve shapes are similar, indicating that the addition of BXFJ and SXFJ will not change the electrochemical corrosion reaction mechanism of the electrode. From Table 1, it can be observed that the $_{Icoor}$ decreases with the increase of the dosage of the four Schiff base corrosion inhibitors, indicating that BXFJ and SXFJ have a corrosion inhibition effect and an increase in corrosion inhibition efficiency. The shape change of the yin and yang regions of the polarization curve is relatively small, and the polarization curve moves towards the direction of decreasing current density. The cathodic Tafel slope $_{bc}$ and anodic Tafel slope $_{ba}$ showed no significant changes, indicating that the corrosion inhibitor forms a corrosion inhibitor film on the surface of carbon steel, slowing down the anodic dissolution and cathodic hydrogen evolution reaction of the steel. The trend of polarization curve changes is consistent with the weight loss test results.

3.3. Resistance Impedance Results

Figure 4 shows the electrochemical impedance spectroscopy (EIS) of Q235 steel in 1 mol/L hydrochloric acid solution with different concentrations (5, 15, 25mg/L) of BXFJ and SXFJ added at room temperature.

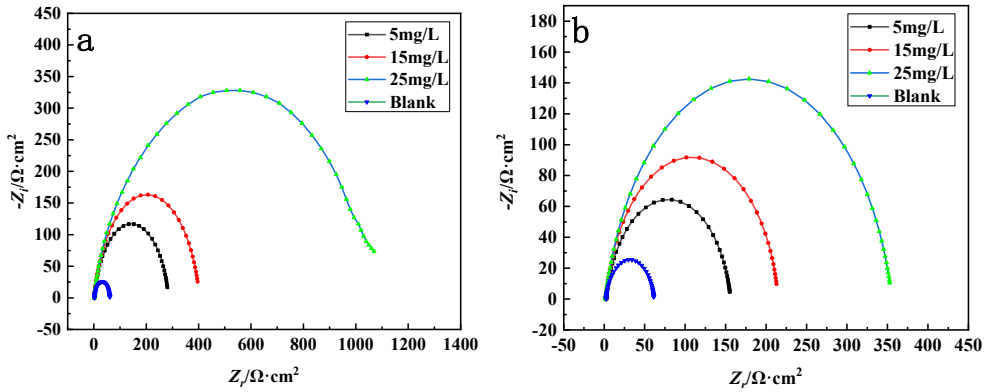

Figure 4. Nyquist of Q235 steel in 1 M HCl solution with different concentration of Schiff base. (a) BXFJ; (b) SXFJ

From Figure 4, it can be seen that Q235 steel exhibits similar capacitance rings in both hydrochloric acid solutions without and with the addition of two corrosion inhibitors, indicating that the corrosion reaction is mainly controlled by the charge transfer step at the metal solution interface, and the diameter of the capacitance ring without the addition of corrosion inhibitor is smaller than that of the capacitance ring with corrosion inhibitor. As the concentration of corrosion inhibitor increases, the diameter of the capacitance ring also increases, indicating that the corrosion reaction of Q235 steel is

inhibited and the effect is enhanced. In addition, the frequency dispersion and non-uniformity of the electrode surface lead to imperfect arc-shaped properties after adding corrosion inhibitors [11].

3.4. Frontline Orbital Theory

The electron distribution of HOMO and LUMO in the frontier molecular orbitals is beneficial for studying the adsorption activity of four corrosion inhibitor molecules, which is related to the molecular electron donating and electron receiving abilities. The frontier orbitals of molecules can be divided into two aspects, namely the highest occupied orbital (HOMO) and the lowest space orbital (LUMO).

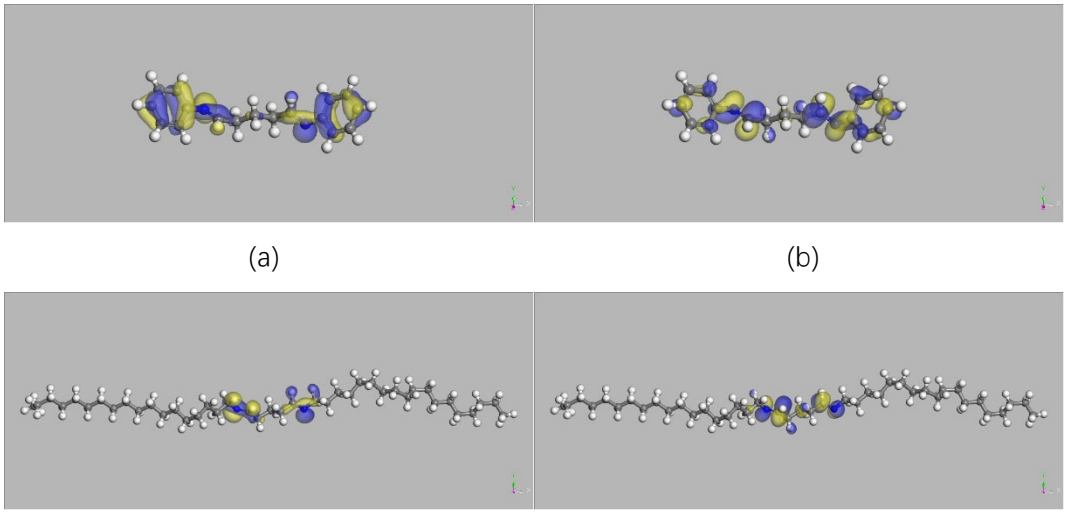

Figure 5. HOMO and LUMO of BXFJ (a, b), SXFJ (c, d)

Table 2. Quantum chemical parameters of BXFJ and SXFJ

	BXFJ	SXFJ
EHOMO(eV)	-5.31169	-5.46413
ELUMO(eV)	-1.290663913	-0.937405519
ΔE(eV)	3.4569	4.5261
μ(eV)	-2.8939	-3.1926
ηa(eV)	1.7285	2.2631
S(eV-1)	0.5785	0.4419

From the data in Table 2, it can be seen that the Δ E values of the two Schiff base corrosion inhibitors, BXFJ, are smaller than SXFJ. The magnitude of the Δ E value can determine the stability of the molecules. The larger the Δ E value, the more stable the molecules are and the less likely they are to adhere to metals The smaller the E value, the more active the molecule is and the easier it is to adhere to metals. Therefore, the smaller the Δ E value of a molecule, the better its anti-corrosion effect and corrosion inhibition effect will be [12].

Hardness (η a) BXFJ is smaller than SXFJ, with opposite softness (S) and dipole moment (μ) BXFJ is greater than SXFJ. According to the theory of soft hard acid-base, the Fe ions on the surface of Fe based metals belong to the boundary base and have lower hardness. Therefore, as the softness and hardness of the corrosion inhibitor molecules increase and decrease, they are more likely to coordinate with the empty d orbitals of Fe. Therefore, the corrosion inhibitor molecules with lower hardness have better corrosion inhibition effects.

3.5. Molecular Adsorption State Diagram

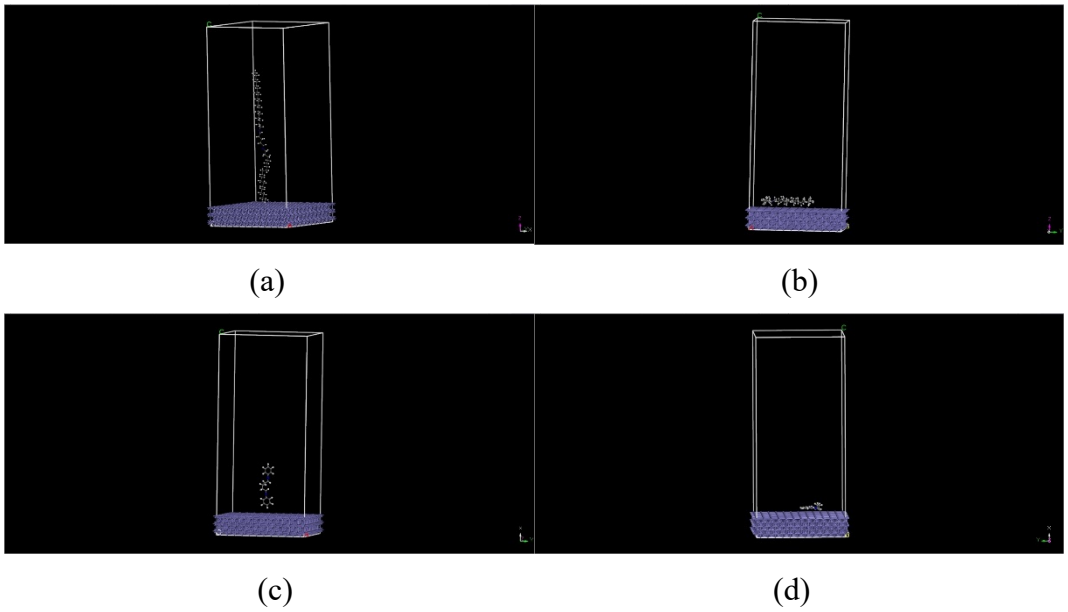

(a) (b)

(c) (d)

Figure 6. Configuration diagram of BXFJ (a, b) and SXFJ (c, d) before and after adsorption on Fe (100) surface

From Figure 6, it can be seen that after the system reaches equilibrium, the N atom and double bond in the corrosion inhibitor molecule are close to the surface of iron, manifested as the five membered ring of OWES, the double bond and nitrogen atom on the five membered ring, the double bond on the branch chain, OWEE's double bond, and N atom are almost parallel to the surface of iron. Both N atoms and double bonds are the main active centers for adsorption, and their interaction with iron contributes significantly. These two molecules do not contain double bonds, and the N atom's branches do not adsorb parallel to the iron surface, forming a certain angle with the metal atom surface. Both corrosion inhibitor molecules can form a protective film on the metal surface, effectively isolating the contact between the iron surface and corrosive substances, thereby preventing and delaying the corrosion of iron.

3.6. Calculation of Adsorption Energy

The adsorption energies of BXFJ and SXFJ are shown in Table 2.

Table 3. The calculated absorption energy

molecule	Etotal (Kcal/mol)	Emolecule (Kcal/mol)	Esurface (Kcal/mol)	Eadsorption (Kcal/mol)
BXFJ	-164461.51	28.03	-164069.75	-419.79
SXFJ	-164268.08	97.26	-164038.75	-326.59

From Table 3, it can be seen that the adsorption energies of the obtained corrosion inhibitors are all negative, indicating that there is interaction between the two corrosion inhibitor molecules and the metal surface, and the two corrosion inhibitors undergo chemical adsorption on the iron surface [13]; Secondly, the larger the absolute value of adsorption energy, the better the corrosion inhibition effect [14]. The absolute value of adsorption energy of BXFJ is greater than that of SXFJ, indicating that BXFJ has better corrosion inhibition effect and stronger adsorption effect than SXFJ, which slows down the corrosion rate of metals. Therefore, BXFJ has stronger ability to inhibit metal corrosion.

4. CONCLUSION

(1) The results of the weight loss method indicate that both corrosion inhibitors have certain corrosion inhibition effects; as the concentration of the corrosion inhibitor increases, the corrosion inhibition efficiency increases, and the corrosion inhibition effect of BXFJ is better.

(2) The polarization curve results indicate that the two corrosion inhibitors have similar curve shapes, indicating that the addition of BXFJ and SXFJ will not change the electrochemical corrosion reaction mechanism of the electrode. BXFJ and SXFJ are mixed corrosion inhibitors. The impedance results indicate that the corrosion reaction is mainly controlled by the charge transfer step at the interface of the metal solution.

(3) Quantum chemical calculations and molecular dynamics simulations both indicate that the two corrosion inhibitor molecules can stably adsorb on the surface of Q235 steel. The active sites of the two corrosion inhibitor molecules mainly include C=N double bonds and heteroatoms N.

REFERENCES

[1] Liu Shuai, Wang Yipeng, Wang Shaofeng Several Discussions on Metal Corrosion and Protection Issues [J] Contemporary Chemical Research, 2022 (9): 23-25

[2] Zheng Chaochao Preparation and Performance Study of New Inorganic Corrosion Inhibitors [D]. Southwest University of Petroleum, 2016

[3] R. Farahati, A. Ghaffarinejad S. M. M. Khoshdel, J. Rezania, H. Behzadi, A. Shockravi Synthesis and potential applications of some thiazoles as corrosion inhibitor of copper in 1 M HCl: Experimental and theoretical studies [J] Prog Org. Coat, 2019, 132 (7): 523-532

[4] K. Hu, J. Zhuang, J. Ding, Z. Ma, F. Wang, X. Zeng Influence of biomolecule DNA corrosion inhibitor on carbon steel [J] Corros Sci, 2017, 125 (8): 68-76

[5] H. Tian, W. Li, L. Liu, X. Gao, P. Han, R. Ding, C. Yang, D. Wang Controlled delivery of multi substituted triazole by metal organic framework for effective inhibition of mill steel corrosion in neutral chloride solution [J] Corros Sci, 2018, 131 (2): 1-16

[6] S. Varvara, R. Bostan, O. Bobis, L. G ă In ă, F. Popa, V. Mena, R. SoutoPolicies as a green corrosion inhibitor for bronze in weakly acidic solution [J] Appl Surf Sci, 2017, 426 (12): 1100-1112

[7] He Riyang. Research on the corrosion inhibition performance of amino acid and peptide double Schiff base inhibitors on Q235 steel [D]. Liaoning Normal University, 2023

[8] Wiberg B. Ab Initial Molecular Orbital Theory by W. J. Hehre, L. Radom, P. v. R. Schleyer, and J. A. Pople, John Wiley, New York, 548pp Price: $79.95 (1986) [J] Journal of Computational Chemistry, 1986, 7 (3): 379-379

[9] North T, Phillips C, Mathews S. A semi empirical method of absorption correction [J] Acta Crystallography Section A, 1968, 24 (3): 351-359

[10] Patterson D. Density functional theory of atoms and molecules [J] Annals of Nuclear Energy, 1989, 16 (11): 611-612

[11] Ituen E, Akranta O, James A. Green Anticorrosive Oilfield Chemicals from 5-Hydroxytryptophan and Synergistic Additives for X80 Steel Surface Protection In Academic Well Treatment Fluids [J] Journal of Molecular Liquids, 2016, 224: 408-419

[12] Dong Xiaocheng, Yang Jingyi, Si Yingwei, Xu Xinru Quantum chemical study on the correlation between the composition and corrosion inhibition performance of Mannich base corrosion inhibitors [J] Petroleum Refining and Chemical Industry, 2021, 52 (11): 102-110

[13] Zhou Wenbin, Zhang Zhengyang, Sun Jie, etc Research on oil soluble corrosion inhibitors and their corrosion inhibition mechanisms [J] Liaoning Chemical, 2022, 51 (7): 987-990

[14] Liu Gang, Yu Tao, Ma Jie, etc A study on the action law of CI-1204 water-soluble corrosion inhibitor [J] Journal of China University of Petroleum (Natural Science Edition), 2014, 38 (3): 112-116